Assessing the Potential of Sodium 1-Oxa- nido -dodecaborate NaB 11 H 12 O for Energy Storage

Salem Ould-Amara, Eddy Petit, Sabine Devautour-Vinot, Marc Cretin, Pascal Georges Yot, Umit Bilge Demirci

ACS OMEGA

Article

Cite This: ACS Omega 2018, 3, 12878−12885

http://pubs.acs.org/journal/acsodf

Assessing the Potential of Sodium 1-Oxa-*nido*-dodecaborate $NaB_{11}H_{12}O$ for Energy Storage

Salem Ould-Amara,[†,§] Eddy Petit,[†] Sabine Devautour-Vinot,[‡] Marc Cretin,[†] Pascal Georges Yot,[‡] and Umit Bilge Demirci*[,†]

[†]Institut Européen des Membranes, IEM—UMR 5635, CNRS, ENSCM, Universite de Montpellier, Place Eugène Bataillon, 34090 Montpellier, France

[‡]Institut Charles Gerhardt Montpellier, ICGM—UMR 5253, CNRS, ENSCM, Universite de Montpellier, Place Eugène Bataillon, 34090 Montpellier, France

ABSTRACT: In the recent years, polyborate anions have been considered as possible candidates for energy. In aqueous solutions, they have been studied as either hydrogen carriers or anodic fuels. In the solid state (as an alkali salt), they have been seen as solid electrolytes. Herein, we focus on sodium 1-oxa-*nido*-dodecaborate $NaB_{11}H_{12}O$, a novel possible candidate for the aforementioned applications. The compound is soluble in water, and its stability depends on pH: under acidic conditions, it readily hydrolyzes while liberating hydrogen, and under alkaline conditions, it is stable, which is a feature searched for an anodic fuel. Over bulk platinum, gold, or silver electrode, oxidation takes place. The best performance has been noticed for the silver electrode. In the solid state, $NaB_{11}H_{12}O$ shows Na^+ conductivity at a high temperature of up to 150 °C. All of these properties are presented in detail, and hereafter they are discussed while giving indications of what have to be developed to open up more realistic prospectives for $NaB_{11}H_{12}O$ in energy.

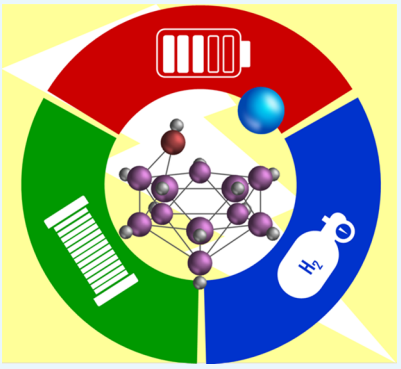

1. INTRODUCTION

Carbon as the main element of fossil fuels has played a central role over the past decades. Nowadays, things are changing and alternative energy sources and carriers are being taken into the 21st century. Carbon will still play a role in the field but any fuel like formic acid and liquid organic carriers will be renewable in order to get closed carbon cycles.[1−3] Search for alternative energy solutions has opened opportunities for compounds made of other elements. Owing to its position in the periodic table against carbon, boron was innately envisaged and, as a matter of fact, boron-based materials have been much investigated since the early 2000s.[4−6]

Boron-based materials have been first seen as liquid-state and solid-state hydrogen carriers. Typical examples are sodium borohydride ($NaBH_4$) and ammonia borane (NH_3BH_3). The former is mainly considered in aqueous solutions in such a way that the couple $NaBH_4$−$4H_2O$ has a maximum gravimetric hydrogen capacity of 7.3 wt % (if the catalyst weight is not taken into account) and the stored hydrogen is released by catalytic hydrolysis.[7] The latter material has been also considered in aqueous solutions for hydrolytic dehydrogenation.[8] However, it is more attractive for solid-state hydrogen storage where most of the stored hydrogen (13 wt %) is generated by thermolytic dehydrocoupling.[9] Many other boron-based materials (most being derivatives of $NaBH_4$ and NH_3BH_3) emerged as possible candidates for hydrogen storage.[4−6] One may cite as uncommon examples the polyborate anions such as nido-$B_{11}H_{14}^-$, closo-$B_{10}H_{10}^{2-}$, and closo-$B_{12}H_{12}^{2-}$; they may be hydrolyzed in the presence of a rhodium-based catalyst at 80 °C.[10]

Boron-based materials like the aforementioned $NaBH_4$ and $NH_3BH_3$are reducing agents. They (as alkaline aqueous solutions) can therefore be used as anodic liquid fuels of direct liquid-fed fuel cells. The former has been much more investigated owing to a higher theoretical specific energy and a lower cost.[11] Yet, the development of the direct borohydride fuel cell is impeded by technical issues, one of them being the "unwanted" heterogeneous hydrolysis of $NaBH_4$ (then, in competition with the expected oxidation).[12] This prompted us to explore the potential of more stable boron-based materials. We first considered the aqueous solution of sodium octahydro-triborate (NaB_3H_8) but, like for $NaBH_4$, heterogeneous hydrolysis took place in some extent. Accordingly, oxidation of $B_3H_8^-$ on platinum and gold electrodes was found to generate effective numbers of electrons of about 5 and 10 out of a theoretical total of 18 electrons.[13] We secondly considered oxidation of the highly stable aqueous solution of sodium dodecahydro-*closo*-dodecaborate ($Na_2B_{12}H_{12}$). It was found to partially oxidize over bulk electrodes (platinum, gold or silver), and much attractively, heterogeneous hydrolysis does not occur.[14]

Boron-based materials have also shown to be potential electrolytic materials of all solid-state Li- or Na-ion batteries. A first example is lithium borohydride ($LiBH_4$). Its hexagonal $P6_3/mmc$ phase, forming at about 110 °C, was found to have a high

Received: August 28, 2018
Accepted: September 26, 2018
Published: October 9, 2018

DOI: 10.1021/acsomega.8b02192
ACS Omega 2018, 3, 12878−12885

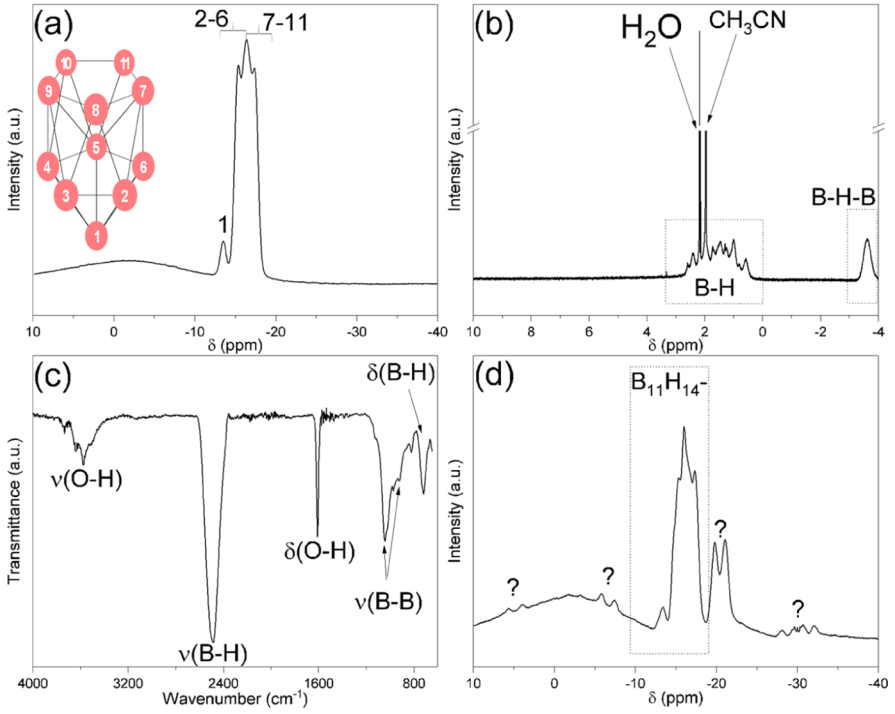

Figure 1. $NaB_{11}H_{14}$: (a) ^{11}B NMR (with the B atoms correlated to the observed peaks) and (b) ^{1}H NMR spectra with CD_3CN/CH_3CN as the solvent; (c) FTIR spectrum; and (d) ^{11}B NMR spectrum of the sample dissolved in alkaline solution (NaOH 0.1 M) and analyzed after 2 h.

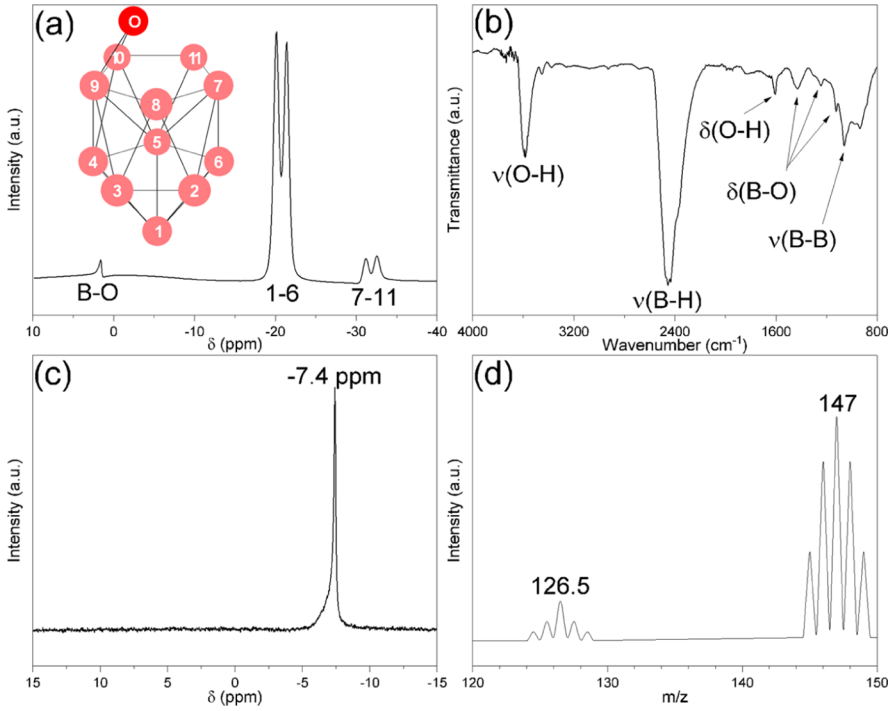

Figure 2. (a) ^{11}B NMR spectrum of $NaB_{11}H_{12}O$ in CD_3CN/CH_3CN (with the B atoms correlated to the observed peaks); (b) FTIR spectrum of solid-state $NaB_{11}H_{12}O$; (c) ^{23}Na NMR spectrum of $NaB_{11}H_{12}O$; (d) mass spectrum of $NaB_{11}H_{12}O$ in aqueous solutions.

electrical conductivity of the order of mS cm^{-1}.[15] High Li^+ conductivity (0.1 mS cm^{-1}) can be achieved at room temperature by confining borohydride in the pores of nanoporous silica.[16] A second example of the boron-based electrolyte is $Na_2B_{12}H_{12}$. The Na^+ conductivity was measured as 100 mS cm^{-1} at 256 °C.[17] Appreciable ionic conductivity (0.5 mS cm^{-1}) was achieved under room conditions for a derivative, $Na_3(BH_4)(B_{12}H_{12})$, made of borohydride and dodecahydro-closo-dodecaborate anions.[18] With such performance, a number of new compounds, most being the derivatives of the aforementioned materials, have been developed.[19]

If the situation is briefly redescribed, it is arguable that boron-based materials have shown to be compounds with prospectives in three energy applications: namely, chemical hydrogen

DOI: 10.1021/acsomega.8b02192
ACS Omega 2018, 3, 12878−12885

storage, anodic fuel of the direct liquid-fed fuel cell, and solid electrolyte of the all-solid battery. Of the materials investigated so far, alkali polyborates have recently emerged and there is a growing interest in them. The present work is viewed in this context. We initially focused on the synthesis of sodium tetradecahydro-*nido*-undecaborate $NaB_{11}H_{14}$ but because it is unstable in the basic medium, we finally focused on the forming derivative, that is, sodium 1-oxa-undecahydro-*nido*-dodecaborate $NaB_{11}H_{12}O$. The compound was properly characterized and its properties related to the aforementioned applications were assessed. The results that are presented herein allow us to position $NaB_{11}H_{12}O$ in the field of energy storage.

2. RESULTS AND DISCUSSION

2.1. Toward $NaB_{11}H_{12}O$. Our preliminary objective was the synthesis of the cluster $NaB_{11}H_{14}$. It was synthesized according to a stepwise process involving $NaBH_4$ as the starting material.[20,21] The ^{11}B NMR spectrum (Figure 1a) is in good agreement with a previously reported one,[22] confirming the successful synthesis of the pure compound. It is worth mentioning the absence of peaks at $\delta > 0$ ppm, discarding then the formation of B−O bonds. The molecular structure of $NaB_{11}H_{14}$ was further verified by ^1H NMR (Figure 2b). All of the signals can be favorably attributed to the 14 hydrogens of the polyborate anion, discarding the presence of any other B−H bond-containing product. The signal of highest intensity at δ 2.3 ppm is attributed to water and the intensity is higher than that of CH_3CN of the anhydrous deuterated solvent (δ 2 ppm). A last analysis of the sample was performed by Fourier transform infrared spectroscopy (FTIR) (Figure 1c). The fingerprint is typical of a compound made of B−B and B−H bonds. The presence of H_2O is confirmed by, for example, the bands at 3800−3200 cm^{-1} (O−H stretching). It is therefore reasonable to attribute these signals to H_2O molecules, complexing the cluster $NaB_{11}H_{14}$.

For a use as the anodic fuel of the direct liquid-fed fuel cell, $NaB_{11}H_{14}$ is expected to be stable in aqueous alkaline solution (NaOH 0.1 M). A solution was prepared (to be stored in an argon-filled glovebox) and the stability was followed by ^{11}B NMR. After 2 h, several new signals at $\delta < -17$ ppm and $\delta > -10$ ppm were observed (Figure 1d), suggesting an evolution of $NaB_{11}H_{14}$ in alkaline solutions. The instability of the anion $B_{11}H_{14}^-$ in aqueous alkaline solutions was reported elsewhere: Ouassas et al. observed the formation of the 1-oxa-undecahydro-*nido*-dodecaborate anion ($B_{11}H_{12}O^-$) by reaction of O_2 with an alkaline solution of $B_{11}H_{14}^-$.[23] Hence, in our conditions, we waited for the complete oxidation of $NaB_{11}H_{14}$. The process took 21 days for a vial stored in the glovebox at room temperature.

The ^{11}B NMR spectrum of the as-formed compound is shown in Figure 2a. It is in good agreement with the molecular structure of the anion $B_{11}H_{12}O^-$.[23] The FTIR spectrum of the oxidation product (Figure 2b) is comparable to that of $NaB_{11}H_{14}$, with the presence of the typical bands for the B−B, B−H, and O−H bonds. There are also small differences that are because of the presence of the B−O bond. NMR analysis of the nucleus ^{23}Na was performed (Figure 2c). The spectrum is featured by only one signal at δ −7.5 ppm. This is in good agreement with a cation Na^+, compensating the negative charge of an inorganic anion.[24] As a last analysis, the molecular weight of the product was determined by mass spectrometry (Figure 2d). An m/z value of 146.8 was found. It is comparable to the molecular weight of $B_{11}H_{12}O^-$ (147 g mol^{-1}), knowing besides that the isotopic pattern score correlates with this anion. Another signal at m/z 126.5 was noted. It is ascribed to $B_{11}H_8^-$, which could be produced by fragmentation of the parent anion during the analysis. To sum up, all of the analyses reported above confirm the complete oxidation of $NaB_{11}H_{14}$ into $NaB_{11}H_{12}O$ when kept in alkaline solution for 21 days.

$NaB_{11}H_{12}O$ is a white solid. It is crystalline. Its X-ray diffraction (XRD) pattern is reported herein for the first time (Figure 3). Using the pattern matching based on the

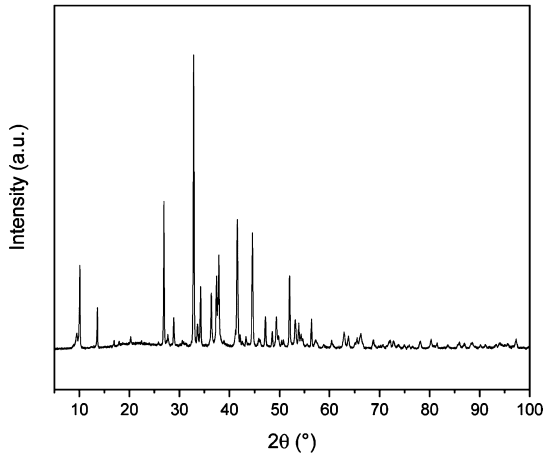

Figure 3. X-ray powder diffraction pattern obtained for $NaB_{11}H_{12}O$ (λ = 1.540059 Å).

PANalytical X'Pert HighScore software and the available crystallographic databases (PDF-4+ v. 4.1403), no matching was found for a screening using the constitutive elements Na, B, O, and H. An extended search including the elements present in the initial reactant revealed traces of both NaCl (ref. pattern 00-001-0993) and $NaOH{\cdot}H_2O$ (ref. pattern 00-002-0706). These observations suggest that the compound is a new crystalline phase. A work is in progress to obtain a sample with a better crystallinity and/or a monocrystal to solve the crystal structure and propose a set of cell parameters.

2.2. Hydrolytic Stability of $NaB_{11}H_{12}O$. The stability of $NaB_{11}H_{12}O$ in aqueous solutions was verified. Though formed in alkaline solution (NaOH 0.1 M), a further test was performed for a higher NaOH concentration. The solid was dissolved in a solution at 1 M NaOH to get a concentration of 10^{-5} M and the as-prepared solution was stored for 25 days under an argon atmosphere (in the glovebox) and at room temperature. No evolution was observed (Figure 4), allowing to go further with this compound as the anodic fuel, that is, for oxidation over bulk metal electrodes.

The stability in the acidic medium was also envisaged. A solution of H_2SO_4 (0.1 M) was prepared. It was used to dissolve $NaB_{11}H_{12}O$. Polyborate anions like $B_{10}H_{10}^{2-}$ and $B_{12}H_{12}^{2-}$ are known to be stable in the acidic medium.[25,26] In contrast, anions like $B_{11}H_{11}^{2-}$, $B_{11}H_{14}^{2-}$, and $B_9H_9^{2-}$ are hydrolytically unstable in the acidic medium.[27,28] In our conditions, $NaB_{11}H_{12}O$ reacted violently in the acidic medium. The reaction was characterized by immediate gas formation: hydrolysis with generation of hydrogen took place. Like, for example, nido-$B_{11}H_{14}^-$,[10] this might open prospectives for chemical hydrogen storage because $NaB_{11}H_{12}O$ carries 6.7 wt % of hydrogen.

2.3. Oxidability of $NaB_{11}H_{12}O$. The stability of $NaB_{11}H_{12}O$ in alkaline solutions is a required property for an anodic fuel. To the authors' knowledge, oxidation of such a compound has not

DOI: 10.1021/acsomega.8b02192
ACS Omega 2018, 3, 12878−12885

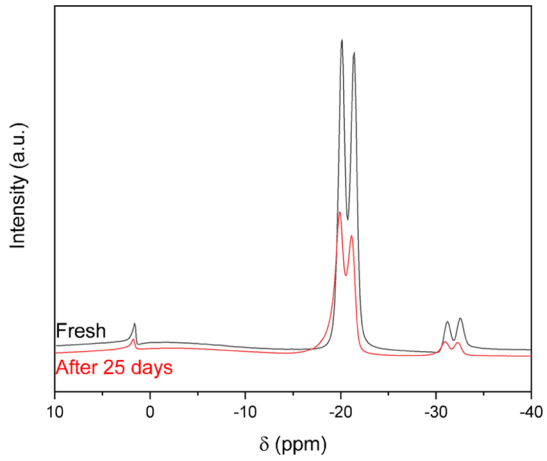

Figure 4. ^{11}B NMR spectra of $NaB_{11}H_{12}O$ (10^{-5} M) in aqueous alkaline (NaOH 1 M) at 0 day (fresh solution) and after 25 days of storage under argon atmosphere and room temperature conditions.

been reported before. The discussion below is thus based on the literature dedicated to $NaBH_4$,[29−31] NaB_3H_8,[13] and $NaB_{12}H_{12}$.[14]

The oxidation of $NaB_{11}H_{12}O$ was first studied by cyclic voltammetry (CV) with bulk platinum as the electrode and under natural diffusion conditions (Figure 5a). The concentration of NaOH was set at 0.1 M and the concentration of the sample at 0.001 M. The voltammogram resembles that recorded for $NaB_{12}H_{12}$ with the same electrode.[14] For the forward scan, there are two oxidation peaks. They are in the region of adsorption/desorption of atomic hydrogen on the electrode surface: a_{Pt1} at −0.73 V versus the saturated calomel electrode (SCE) and a_{Pt2} at −0.6 V versus SCE. Dissociative adsorption of $B_{11}H_{12}O^-$ followed by oxidation of the adsorbed hydrogen H_{ads} would happen. Direct partial oxidation of the anion is also likely to happen. At higher potential, in the region of platinum oxides, there is no oxidation peak, maybe because of electrode poisoning by adsorption of polyborate intermediates or desorption of the same species. For the backward scan, there is one oxidation peak (c_{Pt1}) at −0.69 V versus SCE. It is attributed to the probable oxidation of H_{ads}. The recorded current densities are very low (<2 mA cm^{-2} for e.g. a_{Pt1}). Oxidation of $B_{11}H_{12}O^-$ over the platinum electrode seems to be tough, which might be explained by difficult dissociation of $B_{11}H_{12}O^-$ on the metal surface and/or the absence of direct oxidation. Additional CV experiments were performed with different rotation rates of the platinum rotating electrode (Figure 5b). The oxidation waves were confirmed and the voltammograms were compared to that recorded under natural diffusion conditions. The current densities slightly increased with the increase of the rotation rate. This may be explained by desorption of polyborate intermediates.

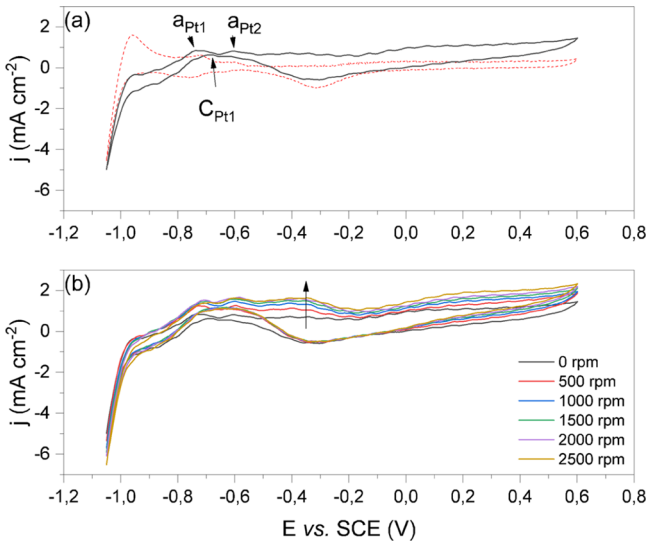

Figure 5. Cyclic voltammograms obtained on platinum (100 mV s^{-1}) for a NaOH 0.1 M solution of $NaB_{11}H_{12}O$ at a concentration of 0.001 M. (a) Under natural diffusion conditions (0 rpm); the voltammogram of 0.1 M NaOH (dashed lines) is shown. (b) Under different rotation rates of the rotating disk electrode (500, 1000, 1500, 2000, and 2500 rpm).

The oxidation of $NaB_{11}H_{12}O$ was then studied by CV with bulk gold as the electrode and under natural diffusion conditions (Figure 6a). The voltammogram shows one oxidation peak at +0.22 V versus SCE (a_{Au1}) during the forward scan and another one at +0.02 V versus SCE (a_{Au2}) during the backward scan. The oxidations are irreversible. They may be ascribed to direct oxidation of $B_{11}H_{12}O^-$ or oxidation of intermediates. The current density of a_{Au1} (3.4 mV cm^{-2}) is slightly higher than that of a_{Pt1} but the oxidation takes place at too positive potential, which makes it less attractive. Gold does not generate current below −0.2 V versus SCE. It would be unable to valorize possibly formed H_{ads} species. The rotation of the electrode (Figure 6b) has a positive effect. The current density for a_{Au1} increases up to 7 mV cm^{-2} at 2500 rpm. Gold is thus less impacted by poisoning from adsorbed polyborate intermediates than platinum is.

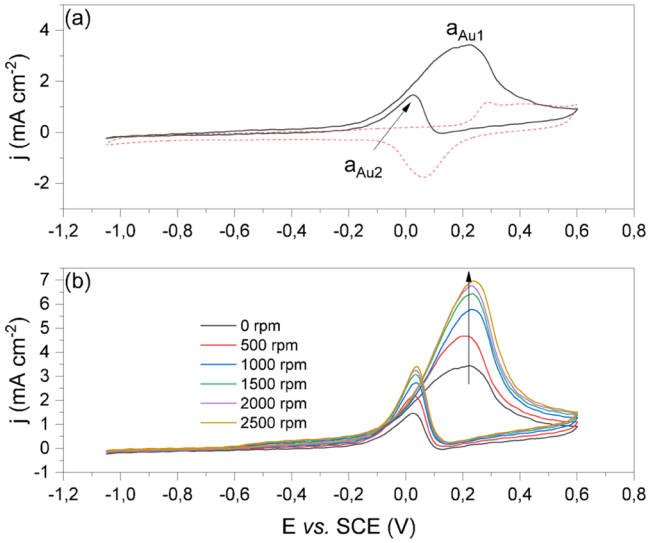

Figure 6. Cyclic voltammograms obtained on gold (100 mV s^{-1}) for a NaOH 0.1 M solution of $NaB_{11}H_{12}O$ at a concentration of 0.001 M. (a) Under natural diffusion conditions (0 rpm); the voltammogram of 0.1 M NaOH (dashed lines) is shown. (b) At different rotation rates of the rotating disk electrode (500, 1000, 1500, 2000, and 2500 rpm).

The oxidation of $NaB_{11}H_{12}O$ was finally studied by CV with bulk silver as the electrode and under natural diffusion conditions (Figure 7a). The forward scan is characterized by two oxidation waves: a_{Ag1} at +0.16 V versus SCE and a_{Ag2} at +0.46 V versus SCE. Direct oxidation of $B_{11}H_{12}O^-$ and/or oxidation of intermediates seems to occur, oxidation being promoted by the formation of surface (hydr)oxides. The

DOI: 10.1021/acsomega.8b02192
ACS Omega 2018, 3, 12878−12885

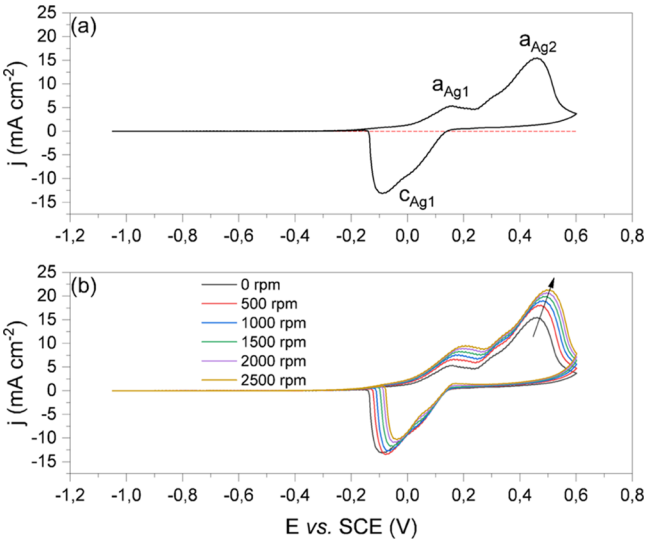

Figure 7. Cyclic voltammograms obtained on silver (100 mV s^{-1}) for a NaOH 0.1 M solution of $NaB_{11}H_{12}O$ at a concentration of 0.001 M. (a) Under natural diffusion conditions (0 rpm); the voltammogram of 0.1 M NaOH (dashed lines) is shown. (b) At different rotation rates of the rotating disk electrode (500, 1000, 1500, 2000, and 2500 rpm).

backward scan is featured by one reduction peak (c_{Ag1}) at +0.1 V versus SCE. It implies that the oxidation process is, at least in part, reversible. The current densities are higher than those measured with the gold and platinum electrodes. For example, the value is 15.5 mA cm^{-2} for a_{Ag2}. Direct and potentially more complete oxidation of $B_{11}H_{12}O^-$ is feasible on silver. At different rotation rates of the rotating silver electrode (Figure 7b), the aforementioned oxidation and reduction processes were confirmed. The current densities were found to slightly increase with, for example, 21.3 mA cm^{-2} at 2500 rpm for a_{Ag2}. This suggests that the electrode would be less impacted by surface poisoning caused by adsorbed oxidation/reduction intermediates.

The best electrode is bulk silver when the electrochemical activity (i.e. current density) is considered only. Oxidation takes place at high potential; this is not really attractive for an anodic fuel. From a fundamental point of view, this shows that oxidation occurs in the metal-oxide region. Like for the anion $B_{12}H_{12}^{2-}$,[14] these results demonstrate the critical role of surface (hydr)-oxides in direct oxidation of $B_{11}H_{12}O^-$. The challenge would then be to develop multimetallic silver-based catalysts showing decreased oxidation potentials. If $B_{11}H_{12}O^-$ is compared to the anion $B_{12}H_{12}^{2-}$, it has a lower electrochemical activity.

The oxidation products were qualitatively analyzed by mass spectrometry. Additional CV experiments were performed for each electrode: 1000 cycles where the potential was positively scanned from −1.05 to +0.6 V versus SCE (no reverse scan) were realized. A fraction of the electrolyte (1 mL) was collected every 100 cycles for analysis. The analyzed fractions revealed the presence of several m/z values, indicating then a complex composition. The possible species corresponding to these values were tentatively denoted on the basis of the available literature.[32−38] The results are summarized in Table 1. For the platinum electrode, six different species were detected but the predominant one is $B_{11}H_{10}O^-$, which presumably forms by oxidation of one of the H of $B_{11}H_{12}O^-$

$$B_{11}H_{12}O^- + OH^- \rightarrow B_{11}H_{10}O^- + H_2O + 2e^- \quad (1)$$

Table 1. Summary of the MS Results for the Electrolytes Analyzed Every 100 Cycles of Positive Scans between −1.05 to +0.6 V vs SCE and for Each of the Electrodes (Platinum, Gold, Silver)[a]

m/z	species	Pt	Au	Ag
85.8	$B_7H_{10}^-$		•	•
98.2	$B_7H_7O^-$		••	••
99.2	$B_7H_8O^-$	•		
102.3	$B_7H_{11}O^-$	••		
113	$B_8H_{10}O^-$		•••	•••
116.8	?	•		
144	$B_{11}H_9O^-$	••		
145.8	$B_{11}H_{10}O^-$	•••		
163	$B_{11}H_{12}O_2^-$	•		

[a]The detected species are given on the basis of their m/z values and are tentatively identified. The relative importance of each is given with • as very minor product, •• as minor product, and ••• as major/predominant product. For clarity, the m/z values corresponding to $B_{11}H_{12}O^-$ are not shown. The signal with m/z 116.8 has not been identified.

Partial oxidative degradation is a minor path for this electrode. The product identification allows better understanding of the low electrochemical activity of platinum, which would be mainly associated to oxidation of H_{ads}. With respect to the gold and silver electrodes, less and different species are formed. Three were detected and identified: $B_8H_{10}O^- > B_7H_7O^- > B_7H_{10}^-$. The formation of the most abundant product $B_8H_{10}O^-$ may be proposed to take place as follows

$$B_{11}H_{12}O^- + 14OH^- \rightarrow B_8H_{10}O^- + 3B(OH)_4^- + 2H_2O + 11e^- \quad (2)$$

Some partial oxidative degradation of $B_{11}H_{12}O^-$ occurred on gold and silver. These observations are in agreement with the CV results obtained with the three electrodes (Figures 5−7).

2.4. Ionic Conductivity of $NaB_{11}H_{12}O$. Recently Duchêne et al. reported a stable 3 V sodium-ion battery based on the use of a solid-state mixed polyborate, namely $Na_2(B_{12}H_{12})_{0.5}(B_{10}H_{10})_{0.5}$, as the electrolyte.[39,40] The use of this material was motivated by an excellent thermal stability up to 300 °C and a high Na^+ conductivity of 0.9 mS cm^{-1} at 20 °C. This is a promising achievement that follows one of the first works about the use of thermally and (electro)chemically stable sodium polyborates (e.g. $Na_2B_{12}H_{12}$) as potential solid-state electrolytes.[17−19]

We measured ionic conductivities of $NaB_{11}H_{12}O$ by using a broadband impedance spectrometer in a range of frequency varying from 0.01 Hz and 1 MHz, with an applied ac voltage of 1 V, and for temperatures from 150 to 0 °C. The results are shown in Figure 8a. Typically, the real part of the ac conductivity, $\sigma(\omega,T)$, results from the combination of three contributions

$$\sigma(\omega, T) = \sigma_{MWS}(\omega, T) + \sigma_{dc}(T) + \sigma'(\omega, T) \quad (3)$$

The polarization component $\sigma'(\omega,T)$, corresponding to the increasing part of the signal observed at high frequency, arises from the local rearrangement of the Na^+ charges causing dipolar reorientation. It is preponderant in the electrical response recorded in the lower temperature domain. The dc conductivity plateau $\sigma_{dc}(T)$, resulting from the long-range redistribution of the Na^+ ions, dominates the intermediate frequency region. Its contribution increases with the temperature, in agreement with a

DOI: 10.1021/acsomega.8b02192
ACS Omega 2018, 3, 12878−12885

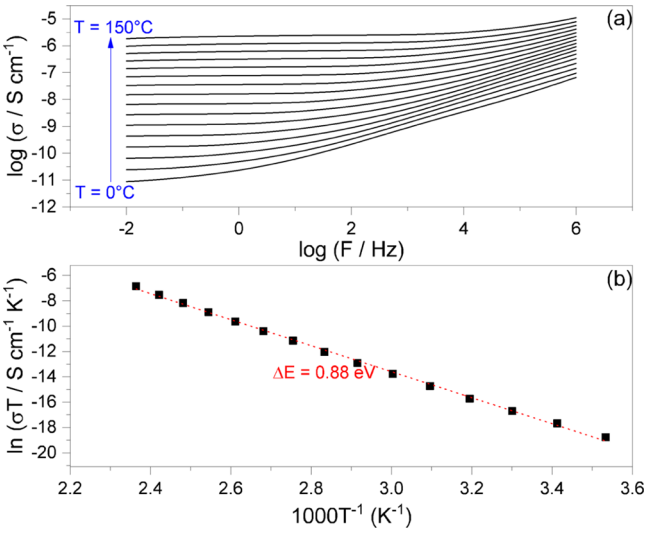

Figure 8. (a) Bode representation of the conductivity vs the frequency in the logarithm scale recorded at temperatures varying from 150 to 0 °C. (b) Corresponding Arrhenius plot of conductivity recorded for $NaB_{11}H_{12}O$; the dashed line corresponds to the linear least-square fit.

thermally activated process. The Maxwell Wagner Sillars contribution $\sigma_{MWS}(\omega,T)$, corresponding to the signal decrease at a low frequency, is only observed for data recorded at high temperatures. It is because of the charge accumulation at the sample/electrode interface and actually supports the ionic features of the charge carriers. Compared to $Na_2B_{12}H_{12}$,[17] the conductivity performances of $NaB_{11}H_{12}O$ are comparable ($\sigma < 10^{-5}$ S cm^{-1} at $T > 150$ °C). However, unlike other sodium polyborates (e.g. $NaB_{11}H_{14}$ with σ between 10^{-2} and 10^{-1} S cm^{-1} at 90−160 °C, and $Na_2B_{10}H_{10}$ with ca. 8×10^{-2} S cm^{-1} at 150 °C),[41,42] the conductivity performances of $NaB_{11}H_{12}O$ are quite low in relation with a lower density and/or lower mobility of the charge carriers. This point is confirmed by the determination of the activation energy (E_a) associated with the ionic transport process. It was deduced from the linear fitting of $\ln(\sigma \times T)$ versus $1/T$ (Figure 8b), according to the Arrhenius equation

$$\sigma(T) = \sigma_0/T \times \exp(-E_a/kT) \quad (4)$$

The energy E_a corresponds to 0.88 eV. It is higher than that reported for the other super-conducting sodium polyborates (0.41 eV for $NaB_{11}H_{14}$, and 0.47 eV for $Na_2B_{10}H_{10}$).[41,42]

The conduction properties of $NaB_{11}H_{12}O$ are comparable to those reported for $Na_2B_{12}H_{12}$,[17] and for both compounds, the conduction properties confine to high temperatures (<150 °C). Better performance could be achieved through the development of new materials (derivatives) based on $NaB_{11}H_{12}O$, as it was in fact done for $Na_2B_{12}H_{12}$ with $Na_3(BH_4)B_{12}H_{12}$.[18]

3. CONCLUSION

In the present work, sodium tetradecahydro-*nido*-undecaborate $NaB_{11}H_{14}$ was first synthesized but it is unstable in the basic medium. It slowly oxidizes into another alkali polyborate, namely, sodium 1-oxa-*nido*-dodecaborate $NaB_{11}H_{12}O$. This alkali polyborate was then characterized and assessed as the potential material for energy storage:

(i) $NaB_{11}H_{12}O$ is not stable in the acidic medium. It hydrolyzes while liberating hydrogen. It could be seen as the potential chemical hydrogen storage material (i.e. hydrogen carrier), provided acidic water is used for hydrolysis or metal-based catalysts are developed to accelerate the kinetics.

(ii) $NaB_{11}H_{12}O$ in an aqueous alkaline solution is hardly oxidized over a bulk platinum electrode. The electrochemical activity is low, with less than 2 mA cm^{-2} (at −0.73 V vs SCE). Better activity is achieved with gold and above all silver. The current density is higher than 15.5 mA cm^{-2} under natural diffusion conditions with the latter electrode. Direct partial oxidation of the anion $B_{11}H_{12}O^-$ (or of intermediates) is likely to occur but the process takes place at a high potential. Further works are necessary to improve the electrocatalytic activity of silver, for example by combining it with other metals toward the formation of multimetallic nanosized electrocatalysts.

(iii) The conductivity of solid-state $NaB_{11}H_{12}O$ was measured between 0 and 150 °C. It is low, with $\sigma < 10^{-5}$ S cm^{-1} at $T < 150$ °C. The conduction activation energy was determined as being 0.88 eV. Improved performances, even at lower temperatures, could nevertheless be achieved by chemically modifying/doping $NaB_{11}H_{12}O$.

In conclusion, the hydrolytic, oxidation, and conductivity properties of $NaB_{11}H_{12}O$ have been investigated. It stands out that the compound is not stable in the acidic medium, it is stable in the alkaline medium, it is rather stable toward oxidation (over Pt, Au, and Ag electrodes) in the alkaline medium, and it shows low mobility of the charge carrier Na^+. Though the current performances are below the state of the art, there is a room for improvements for $NaB_{11}H_{12}O$, especially by focusing on the research avenues mentioned above.

4. MATERIALS AND METHODS

The synthesis of $NaB_{11}H_{14}$ was adapted from a protocol reported elsewhere.[20,21] In an argon-filled glovebox (MBraun M200B, O_2 <0.1 ppm, H_2O <0.1 ppm), 15 g of $NaBH_4$ (Sigma-Aldrich) and 100 mL of anhydrous diglyme (Sigma-Aldrich) were transferred into a three-necked round-bottom Schlenk flask. The flask was connected to a vacuum-argon line, a refrigerant, and an addition funnel containing 63 mL of boron trifluoride diethyl etherate $BF_3{\cdot}O(C_2H_5)_2$ (Sigma-Aldrich). The slurry was heated up to 105 °C. The reactant $BF_3{\cdot}O(C_2H_5)_2$ was added dropwise over a period of 6 h. A yellow precipitate was formed

$$17NaBH_4\ (s) + 20BF_3{\cdot}O(C_2H_5)_2\ (l) \rightarrow 2NaB_{11}H_{14}\ (s) + 15NaBF_4\ (s) + 20H_2\ (g) + 20O(C_2H_5)_2\ (l) \quad (5)$$

The precipitate was filtered and heated at 80 °C to evaporate most of the solvent. Because of residual diglyme and impurities, an aqueous solution (1.31 M) of trimethylamine hydrochloride $(CH_3)_3NHCl$ (Sigma-Aldrich) was added onto the precipitate

$$NaB_{11}H_{14}\ (s) + (CH_3)_3NHCl\ (l) \rightarrow (CH_3)_3NHB_{11}H_{14}\ (s) + NaCl\ (aq) \quad (6)$$

Most of the impurities were dissolved in water, whereas the intermediate $(CH_3)_3NHB_{11}H_{14}$ (s) was in the form of a yellow precipitate. A last purification was done by washing with acetone C_3H_6O (Sigma-Aldrich), followed by addition of water at 57 °C (boiling temperature of acetone). Owing to the miscibility of acetone in water and the insolubility of $(CH_3)_3NB_{11}H_{14}$, a pure

DOI: 10.1021/acsomega.8b02192
ACS Omega 2018, 3, 12878−12885

compound was recovered by filtration and drying under vacuum. As a final step, $(CH_3)_3NHB_{11}H_{14}$ (1 g) was reacted with an aqueous solution of NaOH (0.208 g) at 80 °C for 2 h. Cation substitution took place

$$(CH_3)_3NHB_{11}H_{14}\ (s) + Na^+\ (aq) \rightarrow NaB_{11}H_{14}\ (s) + (CH_3)_3NH^+\ (aq) \quad (7)$$

The yield was found to be 80%. The purity was 99%. $NaB_{11}H_{14}$ was not stable in alkaline aqueous solution (NaOH 0.1 M). It evolved into a new product, which was found to be $NaB_{11}H_{12}O$. A complete oxidation of $NaB_{11}H_{14}$ into $NaB_{11}H_{12}O$ took 21 days under an argon atmosphere.

The polyborate anions in aqueous solution were analyzed by nuclear magnetic resonance (NMR) on Bruker AVANCE-300: ^1H (probe head dual $^1H/^{13}C$, 300.13 MHz, CD_3CN, 30 °C), ^{11}B, and ^{23}Na (probe head BBO10, 96.29 and 79.39 MHz, D_2O, 30 °C). In the solid state, $NaB_{11}H_{14}$ and $NaB_{11}H_{12}O$ were analyzed by FTIR (Nicolet IS50 Thermo Fisher Scientific; 128 scans). The crystallinity of $NaB_{11}H_{12}O$ was verified by powder XRD. The experiment was performed on a PANalytical X'Pert diffractometer equipped with an X'Celerator detector. The diffraction pattern was recorded using a monochromatic wavelength (Cu Kα_1 λ = 1.540593 Å) in the 2θ range 5°−100° with an operating voltage of 40 kV and a beam current of 40 mA using 40 kV. The sample in the powder form was placed into a glass capillary (1 mm diameter) sealed to prevent any decomposition under moisture of ambient air.

Oxidation of $NaB_{11}H_{12}O$ was studied by CV using a μAutolab Type III potentiostat using a three-electrode cell. SCE was used as the reference electrode. The platinum wire was used as the counter electrode. Platinum (Ø 2 mm) or gold (Ø 2 mm) or silver (Ø 4 mm) was used as the rotating disk working electrode. Outgassed Milli-Q Water (18.2 MΩ cm, <3 ppb total organic carbon) was used. For any new measurement, the glassware and electrodes were treated with peroxymonosulfuric acid H_2SO_5 (Caro's acid) overnight and carefully washed with Milli-Q water; then the working electrode surfaces were polished with diamond paste. The cell, thermostated at 20 °C, was degassed with argon. In doing oxygen reduction and carbonation of the electrolyte from ambient carbon dioxide was avoided. In order to avoid water splitting, the voltage range was: −1.05 to +0.6 V versus SCE. The electrolyte features were as follows: 0.1 M NaOH and 0.001 M $NaB_{11}H_{12}O$.

Mass spectrometry experiments (MS; Waters Micromass, Wythenshawe, Manchester, UK; Quattro Micro mass spectrometer with electrospray ionization in negative mode) were performed to check the molecular weight of the anion $B_{11}H_{12}O^-$ and to qualitatively analyze the oxidation by-products. Each sample (in solution) was analyzed by direct injection (FIA: flow injection analysis) using a Waters 2695 pump autosampler with a 20 μL loop. The mobile phase was a 50/50 (vol %) mixture of water and acetonitrile (both of HPLC grade). The spectrometer operated at a constant flow rate such as 0.25 mL min^{-1}. The detection conditions were as follows: capillary potential 3.5 kV; cone potential 30 V; source temperature 120 °C; desolvation temperature 450 °C; cone gas flow 50 L h^{-1}; and desolvation gas flow 450 L h^{-1}. The nebulizer gas was N_2. The experimental spectrum of each identified chemical species (the identification being made on the basis of the available literature[32−38] and on assimilating the m/z value to a molecular weight) was then compared to the modeled spectrum (calculated from the supposed molecular weight) to confirm the identification made.

Impedance measurements were performed on a broadband dielectric spectrometer and Novocontrol alpha analyzer, over a frequency range from 0.01 Hz to 1 MHz with an applied ac voltage of 1 V. The temperature of the sample was controlled by the Quatro Novocontrol system. Measurements were collected from 150 to 0 °C on the anhydrous solid, obtained by in situ heating at 150 °C for 2 h. The measurements were performed on a pellet, with 0.5 and 12 mm of thickness and diameter, respectively, and using the two-probe method.

AUTHOR INFORMATION

Corresponding Author

*E-mail: umit.demirci@umontpellier.fr (U.B.D.).

ORCID

Sabine Devautour-Vinot: 0000-0002-3812-7379

Umit Bilge Demirci: 0000-0003-3616-1810

Present Address

§LEMTA—Université de Lorraine—CNRS—UMR 7563, 2 avenue de la Forêt de Haye, TSA60604—54518 Vandoeuvre cedex, France.

Notes

The authors declare no competing financial interest.

ACKNOWLEDGMENTS

This work was partially funded by the French State via the ANR (Agence Nationale de la Recherche) and the program "Investissements d'Avenir" with the reference ANR-10-LABX-05-01. The work was also partially funded by the Région Languedoc-Roussillon and the program "Chercheur(se)s d'Avenir 2013" (project C3/2013 008555).

REFERENCES

(1) Joó, F. Breakthroughs in Hydrogen Storage-Formic Acid as a Sustainable Storage Material for Hydrogen. *ChemSusChem* **2008**, *1*, 805−808.

(2) Preuster, P.; Albert, J. Biogenic formic acid as a green hydrogen carrier. *Energy Technol.* **2018**, *6*, 501−509.

(3) He, T.; Pei, Q.; Chen, P. Liquid organic hydrogen carriers. *J. Energy Chem.* **2015**, *24*, 587−594.

(4) Moussa, G.; Moury, R.; Demirci, U. B.; Şener, T.; Miele, P. Boron-based hydrides for chemical hydrogen storage. *Int. J. Energy Res.* **2013**, *37*, 825−842.

(5) Puszkiel, J.; Garroni, S.; Milanese, C.; Gennari, F.; Klassen, T.; Dornheim, M.; Pistidda, C. Tetrahydroborates: Development and Potential as Hydrogen Storage Medium. *Inorganics* **2017**, *5*, 74.

(6) Demirci, U. B. Sodium borohydride for the near-future energy: a "rough diamond" for Turkey. *Turk. J. Chem.* **2018**, *42*, 193−220.

(7) Brack, P.; Dann, S. E.; Wijayantha, K. G. U. Heterogeneous and homogenous catalysts for hydrogen generation by hydrolysis of aqueous sodium borohydride ($NaBH_4$) solutions. *Energy Sci. Eng.* **2015**, *3*, 173−188.

(8) Badding, C. K.; Soucy, T. L.; Mondschein, J. S.; Schaak, R. E. Metal ruthenate perovskites as heterogeneous catalysts for the hydrolysis of ammonia borane. *ACS Omega* **2018**, *3*, 3501−3506.

(9) Demirci, U. B. Ammonia borane, a material with exceptional properties for chemical hydrogen storage. *Int. J. Hydrogen Energy* **2017**, *42*, 9978−10013.

(10) Safronov, A. V.; Jalisatgi, S. S.; Lee, H. B.; Hawthorne, M. F. Chemical hydrogen storage using polynuclear borane anion salts. *Int. J. Hydrogen Energy* **2011**, *36*, 234−239.

(11) Ong, B. C.; Kamarudin, S. K.; Basri, S. Direct liquid fuel cells: a review. *Int. J. Hydrogen Energy* **2017**, *42*, 10142−10157.

(12) Serov, A.; Zenyuk, I. V.; Arges, C. G.; Chatenet, M. Hot topics in alkaline exchange membrane fuel cells. *J. Power Sources* **2018**, *375*, 149−157.

DOI: 10.1021/acsomega.8b02192
ACS Omega 2018, 3, 12878−12885

(13) Pylypko, S.; Zadick, A.; Chatenet, M.; Miele, P.; Cretin, M.; Demirci, U. B. A preliminary study of sodium octahydrotriborate NaB_3H_8 as potential anodic fuel of direct liquid fuel cell. *J. Power Sources* **2015**, *286*, 10−17.
(14) Pylypko, S.; Ould-Amara, S.; Zadick, A.; Petit, E.; Chatenet, M.; Cretin, M.; Demirci, U. B. The highly stable aqueous solution of sodium dodecahydro-closo-dodecaborate $Na_2B_{12}H_{12}$ as a potential liquid anodic fuel. *Appl. Catal., B* **2018**, *222*, 1−8.
(15) Matsuo, M.; Nakamori, Y.; Orimo, S.-i.; Maekawa, H.; Takamura, H. Lithium superionic conduction in lithium borohydride accompanied by structural transition. *Appl. Phys. Lett.* **2007**, *91*, 224103.
(16) Blanchard, D.; Nale, A.; Sveinbjörnsson, D.; Eggenhuisen, T. M.; Verkuijlen, M. H. W.; Suwarno; Vegge, T.; Kentgens, A. P. M.; de Jongh, P. E. Nanoconfined $LiBH_4$ as a Fast Lithium Ion Conductor. *Adv. Funct. Mater.* **2015**, *25*, 184−192.
(17) Udovic, T. J.; Matsuo, M.; Unemoto, A.; Verdal, N.; Stavila, V.; Skripov, A. V.; Rush, J. J.; Takamura, H.; Orimo, S.-i. Sodium superionic conduction in $Na_2B_{12}H_{12}$. *Chem. Commun.* **2014**, *50*, 3750−3752.
(18) Sadikin, Y.; Brighi, M.; Schouwink, P.; Černý, R. Superionic Conduction of Sodium and Lithium in Anion-Mixed Hydroborates $Na_3BH_4B_{12}H_{12}$ and $(Li_{0.7}Na_{0.3})_3BH_4B_{12}H_{12}$. *Adv. Energy Mater.* **2015**, *5*, 1501016.
(19) Paskevicius, M.; Jepsen, L. H.; Schouwink, P.; Černý, R.; Ravnsbæk, D. B.; Filinchuk, Y.; Dornheim, M.; Besenbacher, F.; Jensen, T. R. Metal borohydrides and derivatives - synthesis, structure and properties. *Chem. Soc. Rev.* **2017**, *46*, 1565−1634.
(20) Dunks, G. B.; Ordonez, K. P. A one-step synthesis of tetradecahydroundecaborate(1-) ion from sodium tetrahydroborate. *Inorg. Chem.* **1978**, *17*, 1514−1516.
(21) Dunks, G. B.; Barker, K.; Hedaya, E.; Hefner, C.; Palmer-Ordonez, K.; Remec, P. Simplified synthesis of decaborane(14) from sodium tetrahydroborate via tetradecahydroundecaborate(1-) ion. *Inorg. Chem.* **1981**, *20*, 1692−1697.
(22) Hosmane, N. S.; Wermer, J. R.; Hong, Z.; Getman, T. D.; Shore, S. G. High yield preparation of the tetradecahydroundecaborate(1-) anion, $[B_{11}H_{14}]^-$, from pentaborane(9). *Inorg. Chem.* **1987**, *26*, 3638−3639.
(23) Ouassas, A.; Fenet, B.; Mongeot, H.; Gautheron, B.; Barday, E.; Frange, B. Oxygen in an electron-deficient borane skeleton: the oxa-nido-dodecaborate anion $[OB_{11}H_{12}]$? *J. Chem. Soc. Chem. Commun.* **1995**, *5*, 1663−1664.
(24) Koller, H.; Engelhardt, G.; Kentgens, A. P. M.; Sauer, J. ^{23}Na NMR Spectroscopy of Solids: Interpretation of Quadrupole Interaction Parameters and Chemical Shifts. *J. Phys. Chem.* **1994**, *98*, 1544−1551.
(25) Muetterties, E. L.; Balthis, J. H.; Chia, Y. T.; Knoth, W. H.; Miller, H. C. Chemistry of Boranes. VIII. Salts and Acids of $B_{10}H_{10}^{-2}$ and $B_{12}{}_{12}{}^{-2}$. *Inorg. Chem.* **1964**, *3*, 444−451.
(26) Grimes, R. N. Boron clusters come of age. *J. Chem. Educ.* **2004**, *81*, 657−672.
(27) Muetterties, E. L. Chemistry of Boranes. VI. Preparation and Structure of $B_{10}H_{14}^-$. *Inorg. Chem.* **1963**, *2*, 647−648.
(28) Klanberg, F.; Muetterties, E. L. Chemistry of Boranes. XXVII. New Polyhedral Borane Anions, $B_9H_9^{2-}$ and $B_{11}H_{11}^{2-}$. *Inorg. Chem.* **1966**, *5*, 1955−1960.
(29) Lima, F. H. B.; Pasqualeti, A. M.; Molina Concha, M. B.; Chatenet, M.; Ticianelli, E. A. Borohydride electrooxidation on Au and Pt electrodes. *Electrochim. Acta* **2012**, *84*, 202−212.
(30) Olu, P.-Y.; Barros, C. R.; Job, N.; Chatenet, M. Electrooxidation of $NaBH_4$ in Alkaline Medium on Well-defined Pt Nanoparticles Deposited onto Flat Glassy Carbon Substrate: Evaluation of the Effects of Pt Nanoparticle Size, Inter-Particle Distance, and Loading. *Electrocatalysis* **2014**, *5*, 288−300.
(31) Olu, P.-Y.; Deschamps, F.; Caldarella, G.; Chatenet, M.; Job, N. Investigation of platinum and palladium as potential anodic catalysts for direct borohydride and ammonia borane fuel cells. *J. Power Sources* **2015**, *297*, 492−503.
(32) Burg, A. B.; Kratzer, R. The Synthesis of Nonaborane, B_9H_{15}. *Inorg. Chem.* **1962**, *1*, 725−730.
(33) Dobson, J.; Keller, P. C.; Schaeffer, R. Boranes. XXIII. Isononaborane-15. *Inorg. Chem.* **1968**, *7*, 399−402.
(34) Remmel, R. J.; Johnson, H. D.; Jaworiwsky, I. S.; Shore, S. G. Preparation and nuclear magnetic resonance studies of the stereochemically nonrigid anions nonahydrotetraborate(1-)-dodecahydropentaborate(1-), undecahydrohexaborate(1-), and dodecahydroheptaborate(1-). Improved syntheses of pentaborane(11) and hexaborane(12). *J. Am. Chem. Soc.* **1975**, *97*, 5395−5403.
(35) Williams, R. E. The polyborane, carborane, carbocation continuum: architectural patterns. *Chem. Rev.* **1992**, *92*, 177−207.
(36) Beall, H.; Gaines, D. F. Mechanistic aspects of boron hydride reactions. *Inorg. Chim. Acta* **1999**, *289*, 1−10.
(37) King, R. B. Defective Vertices in closo-and nido-Borane Polyhedra. *Inorg. Chem.* **2001**, *40*, 6369−6374.
(38) Schlüter, F.; Bernhardt, E. Syntheses and crystal structures of the closo-borates $M_2[B_7H_7]$ and $M[B_7H_8]$ (M = PPh_4, PNP, and $N(n\text{-}Bu_4)$): the missing crystal structure in the series $[B_nH_n]^{2-}$ (n = 6−12). *Inorg. Chem.* **2011**, *50*, 2580−2589.
(39) Duchêne, L.; Kühnel, R.-S.; Rentsch, D.; Remhof, A.; Hagemann, H.; Battaglia, C. A highly stable sodium solid-state electrolyte based on a dodeca/deca-borate equimolar mixture. *Chem. Commun.* **2017**, *53*, 4195−4198.
(40) Duchêne, L.; Kühnel, R.-S.; Stilp, E.; Cuervo Reyes, E.; Remhof, A.; Hagemann, H.; Battaglia, C. A stable 3 V all-solid-state sodium-ion battery based on a closo-borate electrolyte. *Energy Environ. Sci.* **2017**, *10*, 2609−2615.
(41) Tang, W. S.; Dimitrievska, M.; Stavila, V.; Zhou, W.; Wu, H.; Talin, A. A.; Udovic, T. J. Order-disorder transitions and superionic conductivity in the sodium nido-undeca(carba)borates. *Chem. Mater.* **2017**, *29*, 10496−10509.
(42) Udovic, T. J.; Matsuo, M.; Tang, W. S.; Wu, H.; Stavila, V.; Soloninin, A. V.; Skoryunov, R. V.; Babanova, O. A.; Skripov, A. V.; Rush, J. J.; Unemoto, A.; Takamura, H.; Orimo, S.-i. Exceptional Superionic Conductivity in Disordered Sodium Decahydro-closo-decaborate. *Adv. Mater.* **2014**, *26*, 7622−7626.

DOI: 10.1021/acsomega.8b02192
ACS Omega 2018, 3, 12878−12885